Electronic Supplementary Material (ESI) for Nanoscale.

Supporting Information

A 20-core copper(I) nanocluster as electron-hole recombination inhabitor on TiO_2 nanosheet for enhancing photocatalytic H_2 evolution

Yun-Dong Cao,[a] Hui-Ping Hao,[b] Hua-Shi Liu,[a] Di Yin,[a] Ming-Liang Wang,[a] Guang-Gang Gao,*[a] Lin-Lin Fan,[a] and Hong Liu*[a]

a. School of Materials Science and Engineering, University of Jinan, Jinan, 250022, P. R. China.

b. College of Pharmacy, Jiamusi University, Jiamusi 154007, P. R. China.

E-mail: mse_gaogg@ujn.edu.cn; mse_liuh@ujn.edu.cn

Contents

Materials

The metal precursors $Cu(CO_2CH_3)_2 \cdot H_2O$ (98 mol%, Sigma-Aldrich) and copper powder (Aladdin), NH_4VO_3 (99 mol%, Macklin) and titanium butoxide (99 mol%, Macklin) were used without further purification. Ethinylestradiol ligand was purchased from Macklin. Acetonitrile was used as analytical grade and was not further purified. Fluoric acid was obtained from Supelco.

Experimental methods

1. Synthesis of **UJN-Cu_{20}**

UJN-Cu_{20} was prepared by solvothermal technique using acetone as solvent. Based on the principle of disproportionation reaction, 0.0572 g (0.9 mmol) of Cu(0) powder and 0.0615 g (0.308 mmol) of $Cu(OOCCH_3)_2$ salt were simultaneously introduced into the reaction system to produce copper(I) ion. After two hours of stirring in the presence of 0.2994 g (0.5mmol) ethinylestradiol ligand, the reaction system was added with NH_4VO_3 aqueous solution and stirred for 24 hours. After heating at 80 °C for 48 h, golden block crystals can be obtained in a 40% yield.

2. Synthesis of **TiO_2-NS**

TiO_2-NS were synthesized by a modified method.[1] In a typical synthetic procedure, $Ti(OBu)_4$ (5 mL) was carefully added into a 20-mL

Teflon-lined autoclave containing HF (2 mL, 40 wt %), and gently stirred for 30 min. The resulting mixture was treated at 200 °C for 24 h via a solvothermal process. After cooling down to room temperature naturally, the precipitate was collected by centrifugation and alternatively washing with ethanol and deionized water three times, and then dried under vacuum at 80 °C for 12 h.

3. Synthesis of **UJN-Cu_{20}@TiO_2-NS**

The **TiO_2-NS** were dried at 200 ℃ for 1 hour to remove the adsorbed water on the surface. The dried nanosheets were added into the acetone solution of **UJN-Cu_{20}** and quickly stirred at room temperature for 6 hours. During the stirring process, it was observed that the light-yellow solution gradually became transparent and the white precipitate gradually turned yellow, which proved that **UJN-Cu_{20}** was loaded on the surface of **TiO_2-NS**.

Characterization methods

Single-Crystal X-ray Diffraction Analysis measurements were performed on a Rigaku XtaLAB Pro diffractometer with Mo-Kα radiation (λ = 0.71073 Å) at 293 K for **UJN-Cu_{20}**. Data collection and reduction were performed using the program CrysAlisPro[2]. The intensities were corrected for absorption using the empirical method implemented in SCALE3 ABSPACK scaling algorithm. The structures were solved with

intrinsic phasing methods (*SHELXT-2015*)[3], and refined by full-matrix least-squares on F^2 using *OLEX2*,[4] which utilizes the *SHELXL-2015* module.[4] The crystal structures are visualized by DIAMOND 3.2.[5] Crystallographic data of **UJN-Cu$_{20}$** was delivered to the Cambridge Crystallographic Data Centre (CCDC) and assigned No. 2091492.

Powder X-ray diffraction (XRD) was performed using a D8 Discover (Bruker) diffractometer in Bragg-Brentano geometry (Cu Kα radiation, λ = 1.5418 Å). Data was recorded for the 2θ range from 5° to 80° in steps of 0.05° using an integration time of 1 s. The FTIR spectra were measured on a Nicolet 6700 spectrophotometer using KBr pellets in the range of 4000 to 500 cm^{-1}. The X-ray photoelectron spectrum (XPS) was collected on an ESCA-LAB-MKII spectrometer (UK) to confirm the elemental composition and valence states. High-resolution transmission electron microscopy (HR-TEM) images and elemental mapping of the materials were collected on a JEM-2100Plus instrument. The CEL-SPH2N photolysis water system was employed to test the photocatalytic hydrogen production performance of the materials. Transient photocurrent response tests were carried out using a CHI660E electrochemical workstation with a three-electrode system, in which a glassy carbon electrode was used as the working electrode, a platinum wire as the auxiliary electrode, and a Ag/AgCl electrode as the reference electrode. The preparation of the working electrode was based on published literature.[6]

Calculation methods

Combining with the quantum chemistry method in the computer simulation technology, the Dmol3 module in the Materials Studio software package was used for the calculation. The Dmol3 method is widely used as an approach for determination of electronic structures and analysis of orbital electron occupations. The Perdew-Burke-Ernzerhof (PBE) parametrization of the generalized gradient approximation (GGA) was used for the electron exchange and correlation. In the calculation, the double numerical basis set plus orbital polarization function (DNP) was used to process the valence electron wave function. The iterative convergence criteria for energy, gradient, displacement, and Self-Consistent Field (SCF) under Medium accuracy were 22×10^{-5} Hartree, 4×10^{-3} Hartree/Å, 5×10^{-3} Å and 1×10^{-5} Hartree respectively.

Supporting Figures

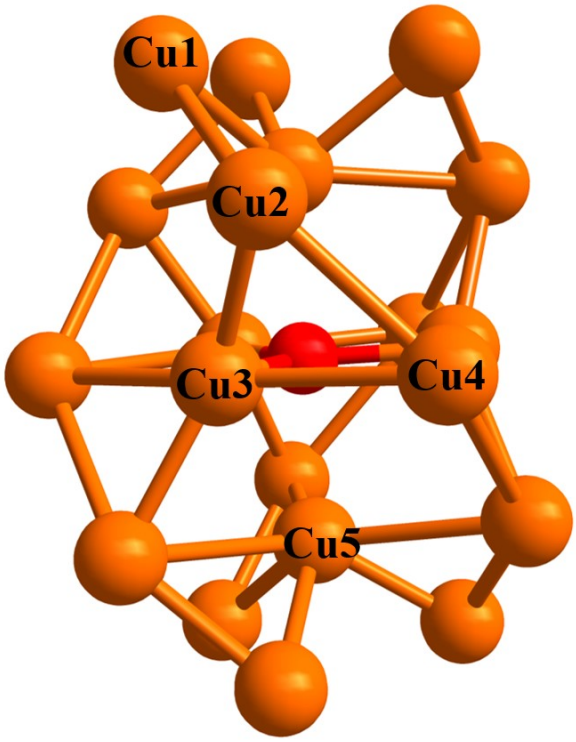

Fig. S1 Ball-stick representation of 20-core copper(I) cluster in **UJN-Cu_{20}** with labels of asymmetric copper atoms.

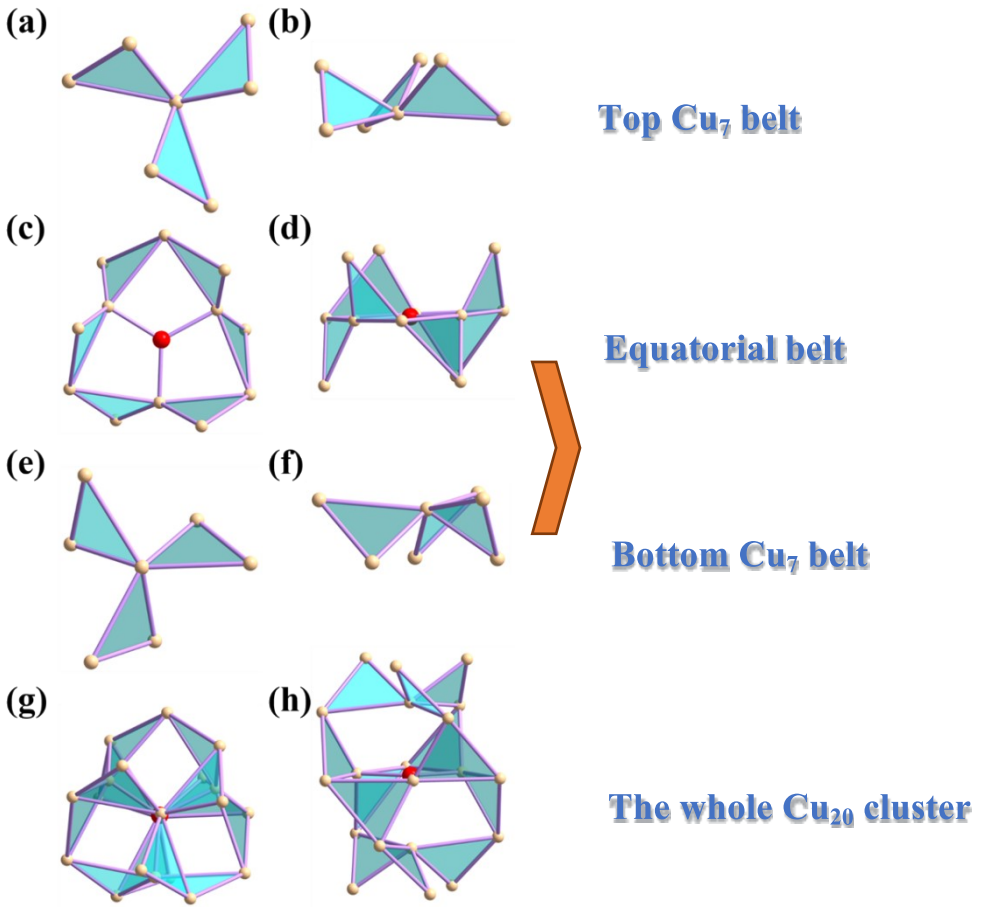

Fig. S2 Top (a, c, e, g) and side (b, d, f, h) views of the Cu_7 belts, equatorial belt, and the whole Cu_{20} cluster in **UJN-Cu$_{20}$** with ligand atoms being omitted for clarity (color codes: Cu, yellow; O, red).

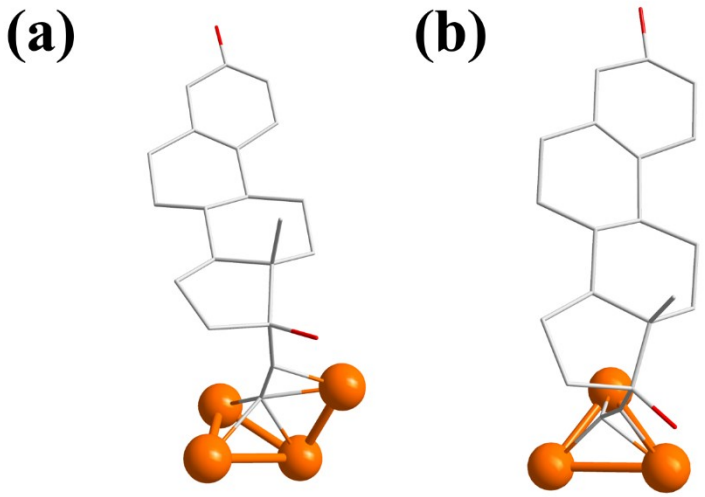

Fig. S3 Coordination mode of ethinylestradiol ligand.

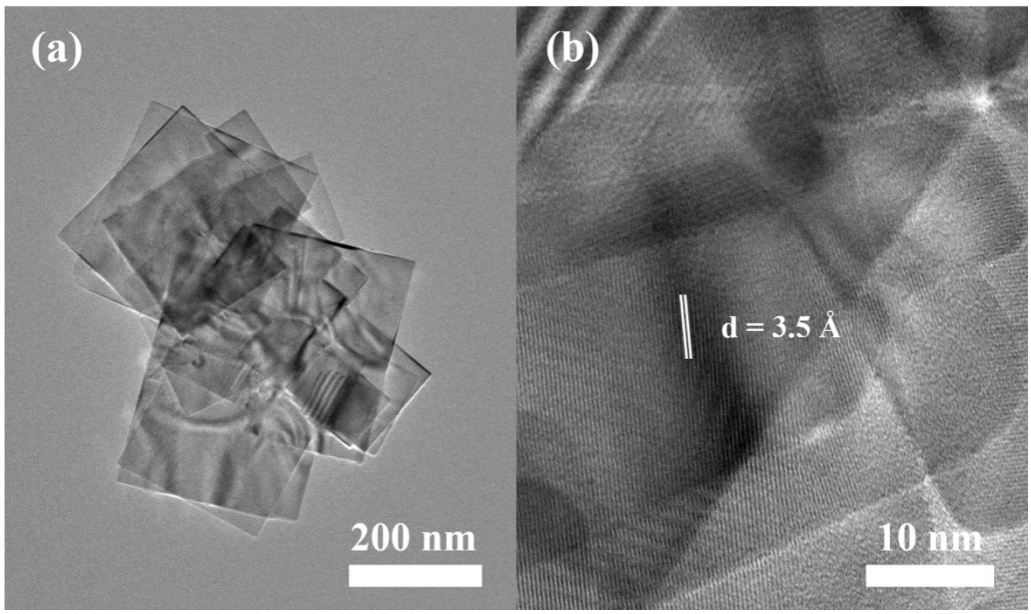

Fig. S4 TEM (a) and HR-TEM (b) images of anatase **TiO_2-NS**.

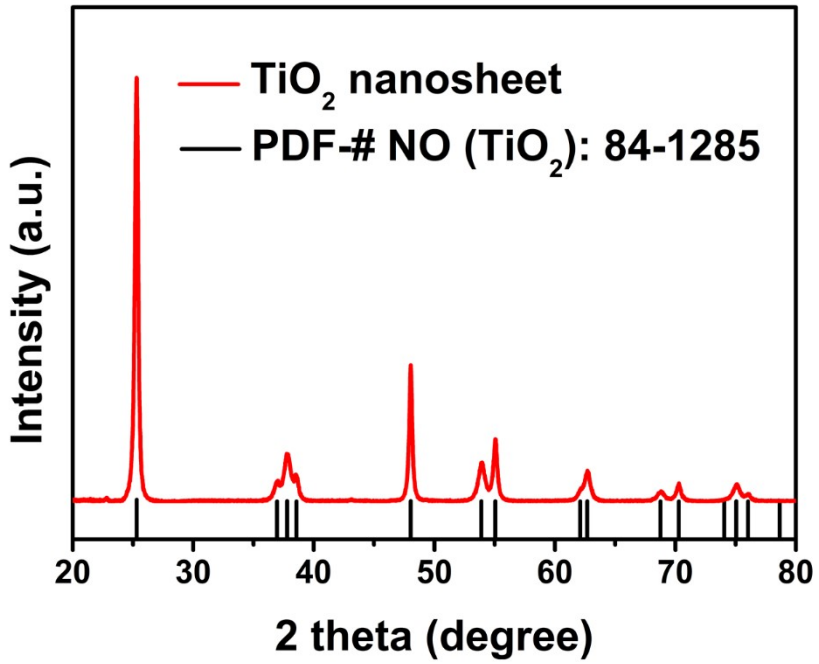

Fig. S5 XRD pattern of **TiO_2-NS** which is consistent with the characteristic peaks of anatase TiO_2.

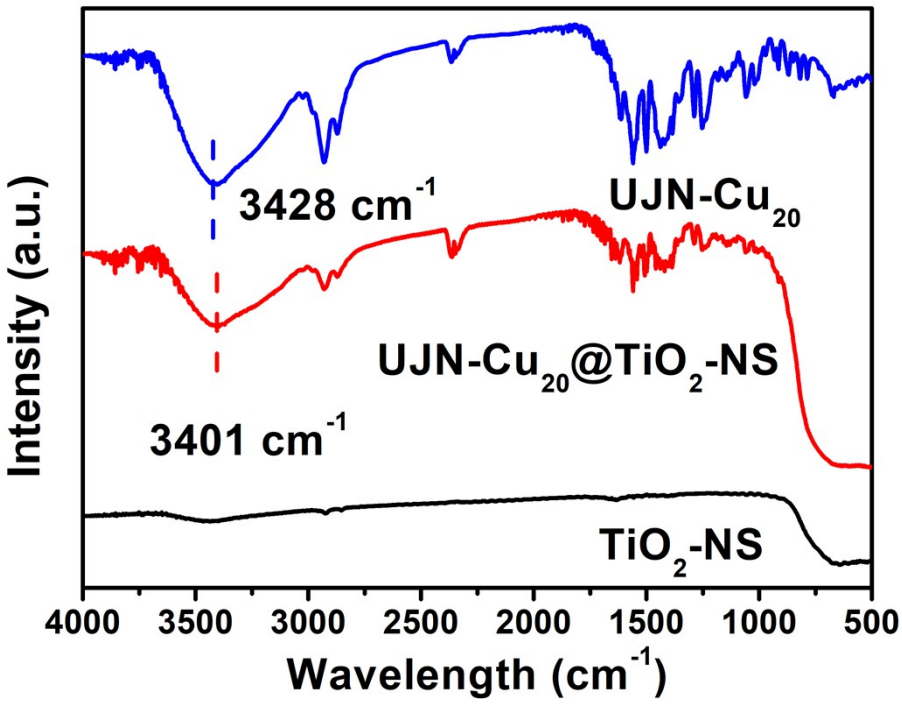

Fig. S6 FTIR spectra of **UJN-Cu$_{20}$**, **UJN-Cu$_{20}$@TiO$_2$-NS**, and **TiO$_2$-NS**.

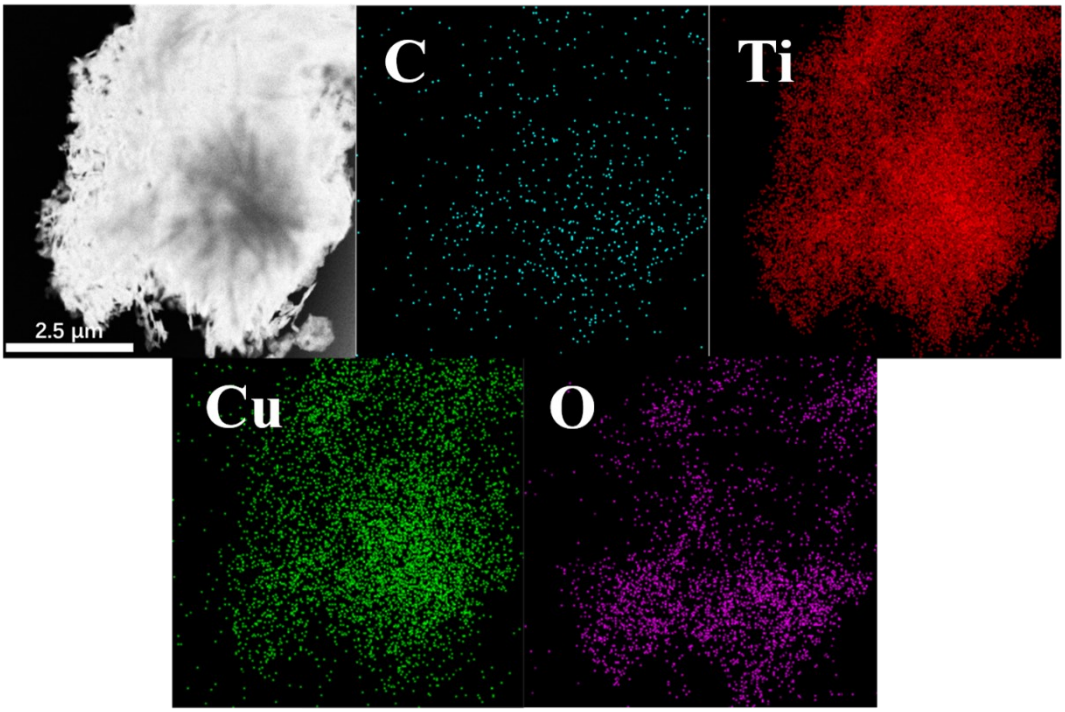

Fig. S7 Elemental mapping images of **UJN-Cu_{20}@TiO_2-NS**.

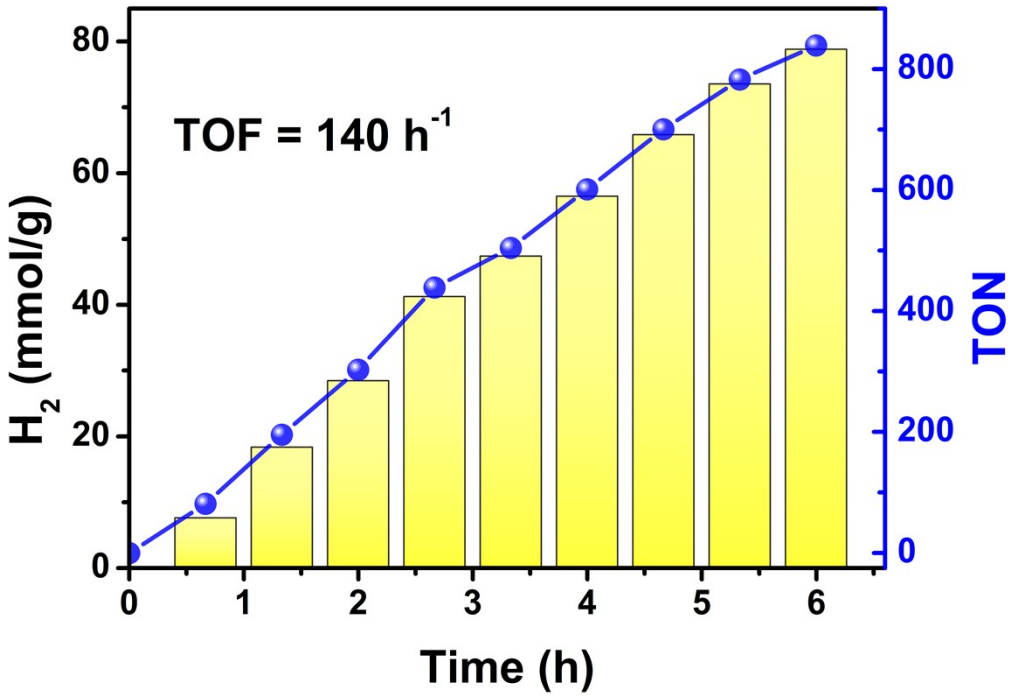

Fig. S8 Turnover numbers and turnover frequency of **UJN-Cu_{20}@TiO_2-NS** catalyst.

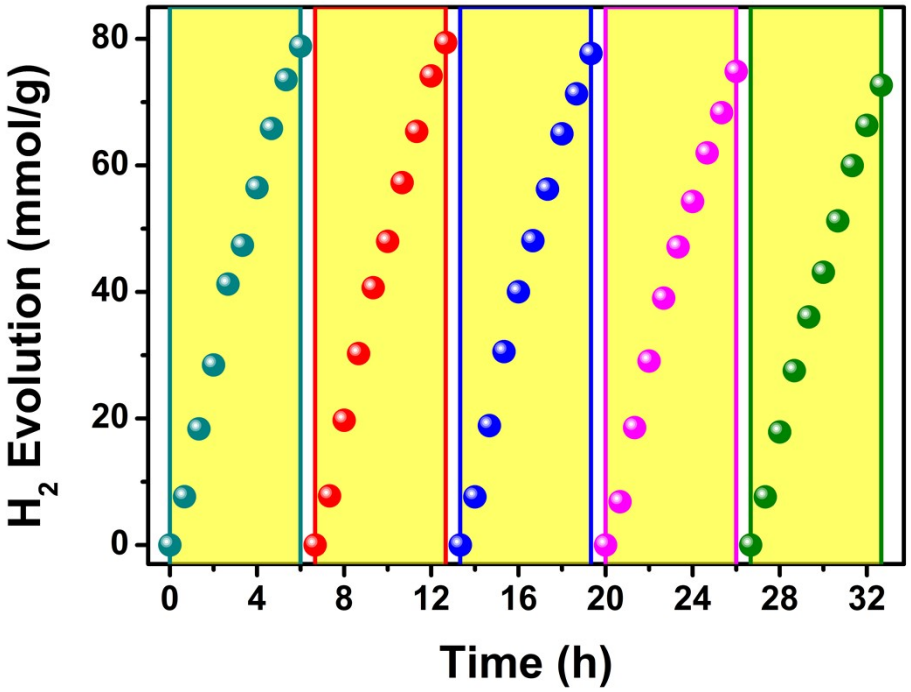

Fig. S9 Stability test of photocatalytic hydrogen evolution of **UJN-Cu_{20}@TiO_2-NS** catalyst.

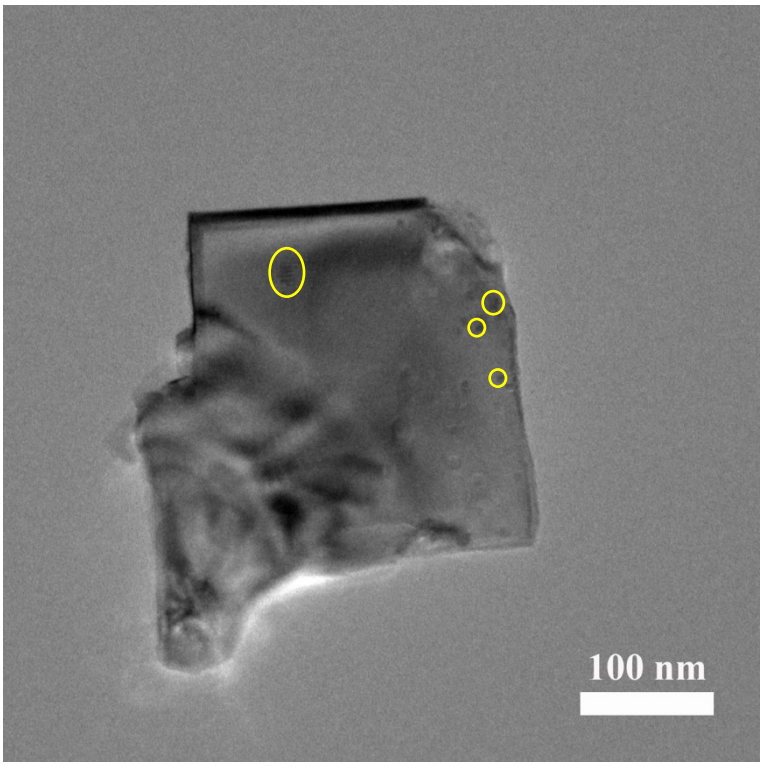

Fig. S10 TEM image of **Cu_{14}@TiO_2-NS**.

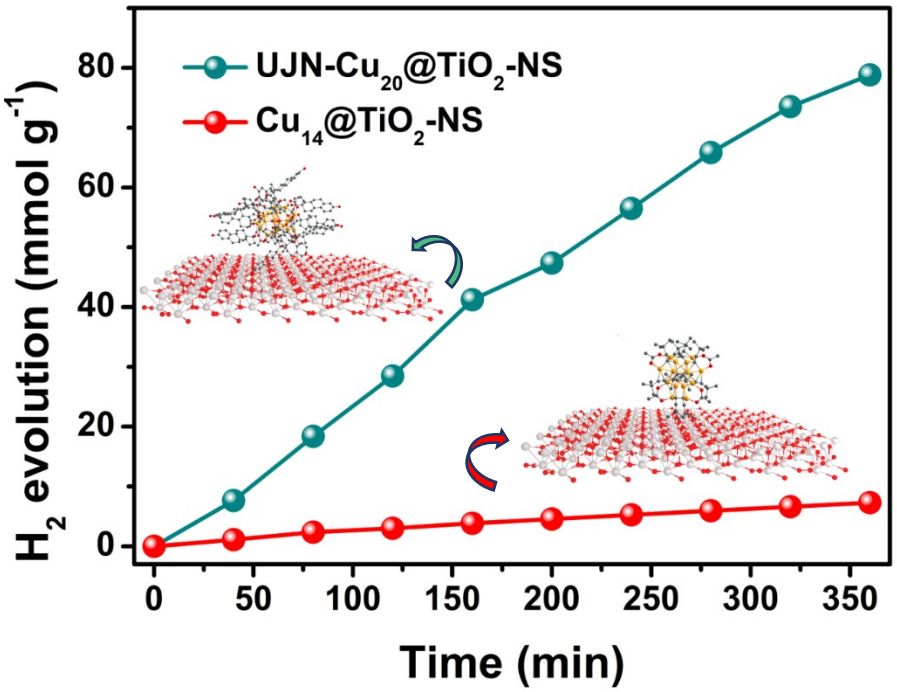

Fig. S11 Comparison of photocatalytic H_2 evolution properties between **UJN-Cu_{20}@TiO_2-NS** and **Cu_{14}@TiO_2-NS**.

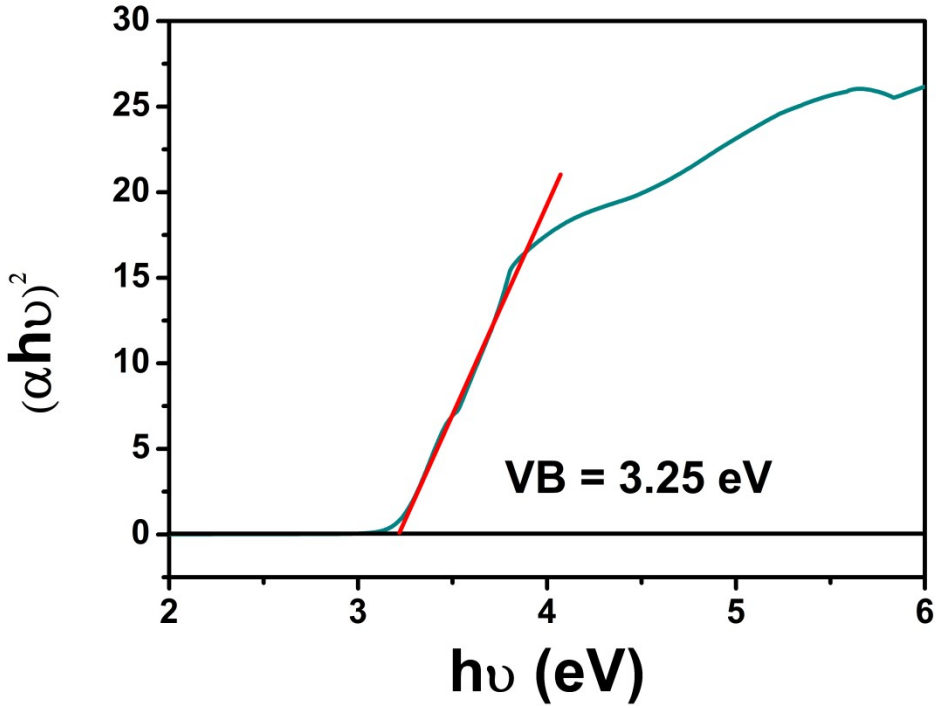

Fig. S12 Band gap of **TiO_2-NS** calculated by UV-visible absorption spectra.

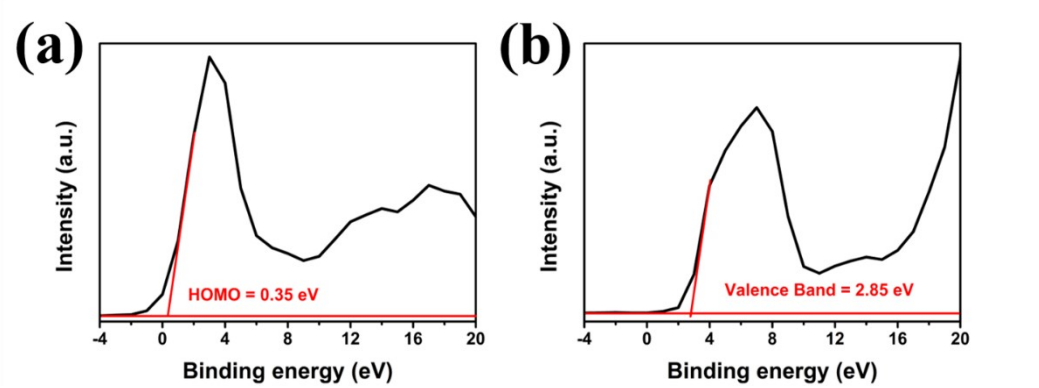

Fig. S13 Valence band XPS spectra of **UJN-Cu$_{20}$** (a) and **TiO$_2$-NS** (b).

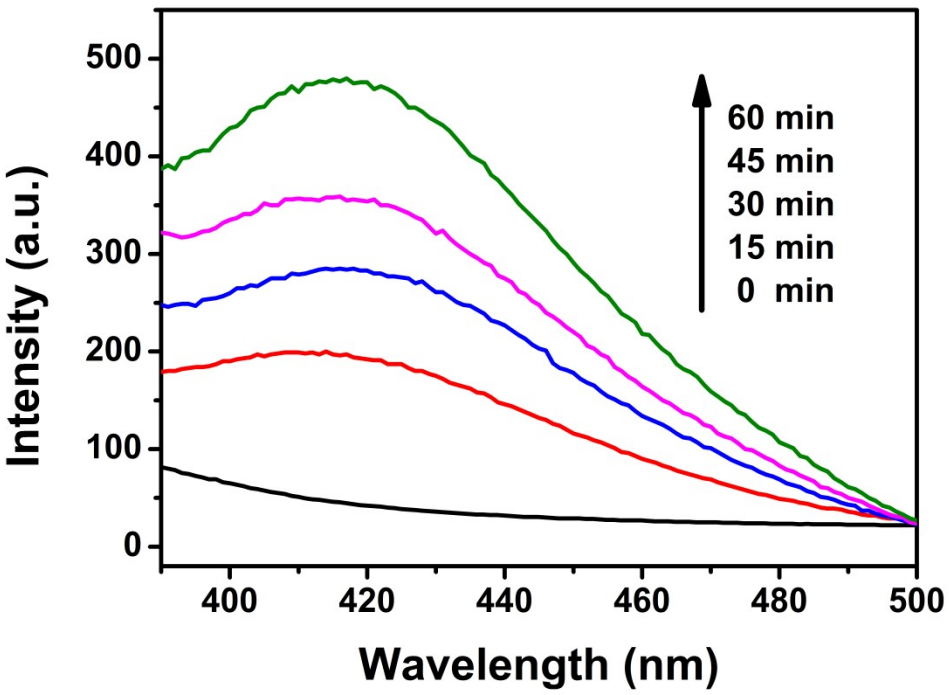

Fig. S14 Fluorescence spectra of terephthalic acid with addition of **UJN-Cu_{20}@TiO_2-NS**.

Reference

(1) X. Han, Q. Kuang, M. Jin, Z. Xie, L. Zheng, *J. Am. Chem. Soc.* **2009**, 131, 3152-3153.

(2) CrysAlisPro 2012, Agilent Technologies. Version 1.171.36.31.

(3) G. M. Sheldrick, *Acta Cryst. A* **2015**, *71*, 3-8.

(4) O. V. Dolomanov, L. J. Bourhis, R. J. Gildea, J. A. K. Howard, H. Puschmann, *J. Appl. Cryst.* **2009**, *42*, 339-341.

(5) K. Brandenburg, Diamond, 2010.

(6) E. J. Popczun, J. R. Mckone, C. G. Read, A. J. Biacchi, A. M. Wiltrout, N. S. Lewis and R. E. Schaak. *J. Am. Chem. Soc.* **2013**, 135, 9267-9270.